Acta Crystallographica Section B
Structural Science
ISSN 0108-7681

Structures of incommensurate and commensurate composite crystals Na_xCuO_2 (x = 1.58, 1.6, 1.62)

Sander van Smaalen,[a]* Robert Dinnebier,[b] Mikhail Sofin[b] and Martin Jansen[b]‡

[a]Laboratory of Crystallography, University of Bayreuth, Bayreuth, Germany, and [b]Max-Planck-Institute for Solid State Research, Heisenbergstrasse 1, D-70569 Stuttgart, Germany

‡ E-mail: jansen@fkf.mpg.de.

Correspondence e-mail: smash@uni-bayreuth.de

Received 23 March 2006
Accepted 26 September 2006

Dedicated to Professor Dr Ing. Hartmut Fuess on the occasion of his 65th birthday

Na_xCuO_2 ($x \simeq 1.6$) has been synthesized for different compositions x, resulting in both commensurate and incommensurate composite crystals. The crystal structures are reported for two incommensurate compounds (x = 1.58 and 1.62) determined by Rietveld refinements against X-ray powder diffraction data. The incommensurate compounds and commensurate $Na_8Cu_5O_{10}$ (x = 1.6) are found to possess similar structures, with valence fluctuations of Cu^{2+}/Cu^{3+} as the origin of the modulations of the CuO_2 subsystems; the displacive modulations of Na being defined by the closest Na—O contacts between the subsystems. A comparison of the structure models obtained from single-crystal X-ray diffraction, synchrotron-radiation X-ray powder diffraction and X-ray powder diffraction with Cu $K\alpha_1$ radiation indicates that single-crystal X-ray diffraction is by far the most accurate method, while powder diffraction with radiation from an X-ray tube provides the least accurate structure model.

1. Introduction

Although high-temperature superconductivity (HTSC) and giant magnetoresistance (GMR), as found in various families of complex oxides, have attracted much attention over past decades, these phenomena are far from being fully understood. In such materials, a specific degree of electron correlation induces an intricate interplay of charge, orbital and spin ordering that constitute the microscopic mechanisms behind the macroscopic responses of HTSC and GMR oxides (Tokura & Nagaosa, 2000). Dealing with such features of the electronic structures of transition metal oxides is a difficult task. Moreover, HTSC and GMR are commonly generated by the extrinsic doping of an ideal parent compound. As a consequence, the periodicities of the crystalline solids are seriously perturbed and in most cases lateral inhomogenities develop that eventually could cause phase separations. Thus, in these cases, crystalline order is lacking, which is an indispensable prerequisite for being able to analyse experimental data measured on extended solids, and to appropriately treat their electronic properties using quantum mechanics.

Against this background, a recently discovered family of mixed-valence sodium oxocuprates (II/III) seems to provide a valuable basis for circumventing the problems mentioned. Since these oxocuprates are doped intrinsically, long-range order is retained, thus allowing for a rational treatment of the crystal structure. Interest in these compounds arises from their electronic properties which are related to the mixed-valence state of copper, with the Cu^{2+}/Cu^{3+} ratio depending on the composition x (Horsch *et al.*, 2005).

As with $NaCuO_2$, which may be regarded as the aristotype of the new family of cuprates of the general composition

Na_xCuO_2, they all contain CuO_2 ribbons formed by trans-edge-sharing CuO_4 squares as the characteristic structural element. Representatives of the compositions $Na_3Cu_2O_4$ (x = 1.5) and $Na_8Cu_5O_{10}$ (x = 1.6) have been obtained as single crystals, and their crystal structures have been determined by single-crystal X-ray diffraction (Sofin *et al.*, 2005). Both compounds show approximately one-dimensional electronic properties, with spin and charge ordering occurring at well separated temperatures around 30 and 500 K, respectively. Most remarkably, the charge ordering is not explicable in terms of the quantum mechanical CDW (charge-density wave) concept, but instead by classical, long-range Coulomb interactions. Thus, $Na_3Cu_2O_4$ and $Na_8Cu_5O_{10}$ are the first unambiguous manifestations of Wigner crystals (Horsch *et al.*, 2005).

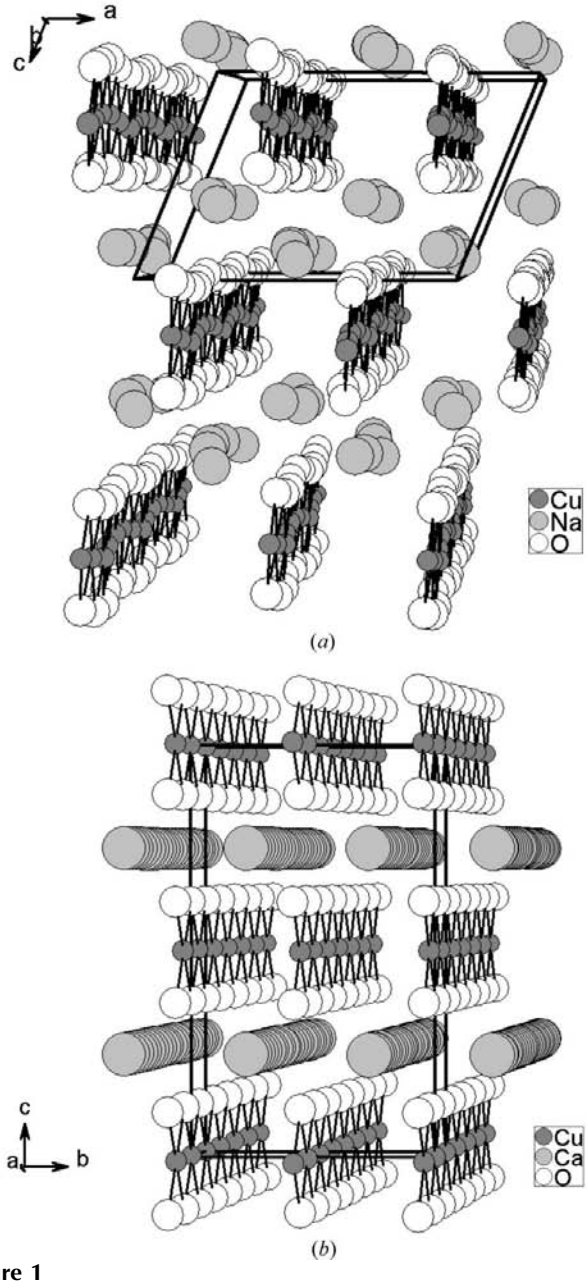

Figure 1
The crystal structure of (*a*) Na_xCuO_2 compared with the structure of (*b*) $Ca_{0.82}CuO_2$ (Miyazaki *et al.*, 2002). A perspective view along the mutually incommensurate chain axes is shown.

$Na_3Cu_2O_4$ (x = 1.5) and $Na_8Cu_5O_{10}$ (x = 1.6) can be considered to be commensurate composite crystals that are described by different unit cells for the CuO_2 and Na subsystems (van Smaalen, 1999). Na_xCuO_2 belongs to the class of incommensurate composite crystals for irrational values of x. They are built of ribbons of CuO_2 and chains of Na ions that run along the **b** axis, with chains of Na ions forming a honeycomb pattern with the voids occupied by cuprate ribbons (Fig. 1*a*). Different periodicities are found along the Na chains and CuO_2 ribbons, with commensurate ratios of 0.75:1 in $Na_3Cu_2O_4$ and 0.8:1 in $Na_8Cu_5O_{10}$. The ratio is an irrational number close to 0.8 for the incommensurate composite compounds reported here.

Na_xCuO_2 ($x \simeq 1.6$) is closely related to incommensurate Ca_yCuO_2 ($y \simeq 0.8$; Siegrist *et al.*, 1990; Miyazaki *et al.*, 2002). Both compounds possess similar ribbons of CuO_2, but these are stacked differently in order to accommodate two chains of Na ions for each ribbon of CuO_2 in Na_xCuO_2, whereas Ca_yCuO_2 contains a single chain of Ca ions (Fig. 1*b*).

The present contribution re-analyses the crystal structure of $Na_8Cu_5O_{10}$ (x = 1.6) as a commensurate composite crystal within the superspace approach (Janssen *et al.*, 1995; van Smaalen, 2004). The incommensurate compounds Na_xCuO_2 have only been obtained as crystalline powders. Therefore, the results of the Rietveld refinements against X-ray powder diffraction data are reported for the crystal structures of the incommensurate composite crystals with x = 1.58 and x = 1.62, respectively.

2. Experimental

2.1. Diffraction experiments

The syntheses of the microcrystalline powders and single crystals have been described elsewhere (Sofin *et al.*, 2005). X-ray powder diffraction was measured on a series of Na_xCuO_2 compounds with $1.56 < x < 1.66$. Samples were loaded into glass capillaries of 0.2 mm diameter. X-ray diffraction measurements were collected at room temperature with a Stoe Stadi-P transmission diffractometer (primary-beam Johansson-type Ge-monochromator for Cu $K\alpha_1$ radiation; linear position-sensitive detector; step size 0.01° 2θ). The composite character of these materials is shown by the diffraction maxima of the CuO_2 subsystem that occur at almost the same diffraction angles in different compounds. The diffraction maxima of the Na subsystem are dependent on the value of x (Fig. 2). The data for x = 1.62 were selected for structural analysis (Table 1).

High-resolution X-ray powder diffraction data were collected for $Na_{1.58}CuO_2$ on the beamline X3B1 of the National Synchrotron Light Source at Brookhaven National Laboratory, Upton, New York. The sample was sealed in a lithium borate glass capillary of diameter 0.3 mm (Hilgenberg glass No. 50). X-rays of wavelength 0.65 Å were selected by a

Table 1
Experimental details.

	$Na_{1.6}CuO_2$†	$Na_{1.58}CuO_2$	$Na_{1.62}CuO_2$
Crystal data			
Chemical formula	$Na_{1.6}CuO_2$	$Na_{1.57664}CuO_2$	$Na_{1.61688}CuO_2$
Chemical formula weight	132.3	131.791	132.716
Temperature (K)	293	293	293
Cell setting, superspace group	Monoclinic, $C2/m(0\sigma_20)s0$	Monoclinic, $C2/m(0\sigma_20)s0$	Monoclinic, $C2/m(0\sigma_20)s0$
Subsystem 1‡	CuO_2	CuO_2	CuO_2
a, b, c (Å)	8.228 (1), 2.7858 (4), 5.707 (1)	8.24153 (4), 2.78589 (2), 5.71687 (3)	8.23682 (15), 2.79269 (4), 5.71224 (10)
β (°)	111.718 (2)	111.9698 (5)	111.6696 (9)
V (Å^3)	121.528	121.727 (1)	122.112 (5)
σ_2	0.8	0.78832 (2)	0.80844 (3)
Z	2	2	2
Subsystem 2‡	Na	Na	Na
a, b, c (Å)	8.228 (1), 3.4823 (5), 5.707 (1)	8.24153 (4), 3.53396 (3), 5.71687 (3)	8.23682 (15), 3.45441 (5), 5.71224 (10)
β (°)	111.718 (2)	111.9698 (5)	111.6696 (9)
V (Å^3)	151.910	154.313 (1)	151.046 (6)
Modulation wavevector	(0, 1.25, 0)	[0, 1.26852 (3), 0]	[0, 1.23695 (3), 0]
Z	4	4	4
D_{calc} (Mg m^{-3})	3.616	3.596	3.609
Data collection			
Radiation type	Mo $K\alpha$†	Synchrotron	Cu $K\alpha_1$
Wavelength (Å)	–	0.65046	1.54059
Specimen form, colour	–	Powder, black	Powder, black
Specimen size (mm)	–	Capillary, 0.3 mm	Capillary, 0.2 mm
Data collection method	–	2θ scan	2θ scan
2θ range (°)	–	5.000–43.404	9.987–79.977
2θ step size (°)	–	0.004	0.01
Refinement			
R_p, R_{wp}	–	0.075, 0.101	0.094, 0.122
R_{Bragg} (all reflections; obs)	0.035	0.047	0.055
Goodness-of-fit	–	2.00	1.95
Excluded region(s)	–	None	None
Profile function	–	Pseudo-Voigt	Pseudo-Voigt
No. of parameters	107	36	37
No. of data points	–	9602	7000
Weighting scheme	–	Based on measured s.u.s	1
$(\Delta/\sigma)_{max}$	–	0.295	–

† The crystal data and data collection data of commensurate $Na_{1.6}CuO_2$ have been taken from Sofin *et al.* (2005). ‡ The description of the first subsystem also provides canonical superspace, with W^1 equal to the unit matrix. The second subsystem is described by the matrix W^2 corresponding to an interchange of **b*** and **q**.

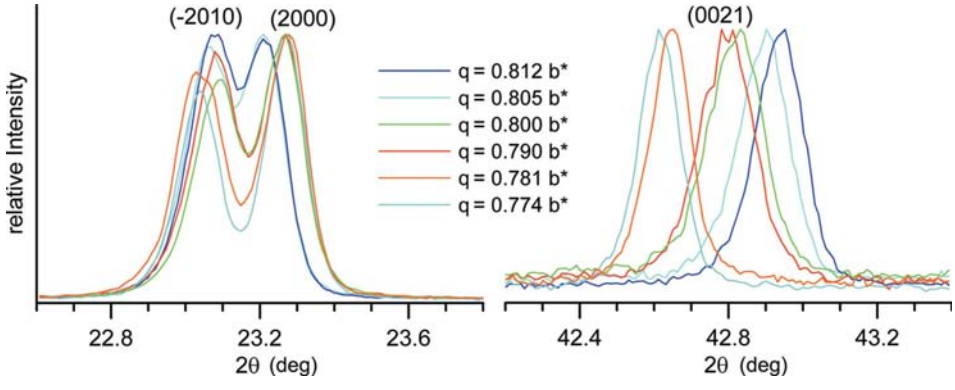

Figure 2
Scattered intensities as a function of the diffraction angle 2θ. (*a*) Around the ($\bar{2}$010) and (2000) peaks common to the subsystems. (*b*) Around the (0021) main reflection of the Na subsystem.

double Si(111) monochromator. Wavelengths and the zero point were determined from eight well defined reflections of the NBS1976 flat-plate alumina standard. The diffracted beam was analyzed with a Ge(111) crystal and detected with a Na(Tl)I scintillation counter employing a pulse height discriminator in the counting chain. The incoming beam was monitored by an ion-chamber for normalization purposes, in order to take into account the decay of the primary beam. Data were taken in steps of 0.004° 2θ from 5.0 to 43.4° 2θ for 3.0 s per step (Table 1). The sample was spun during measurement to obtain better particle statistics. The powder pattern of $Na_{1.58}CuO_2$ exhibits several peaks of small impurity phases, presumably belonging to the same class of substance as the main compound.

Data reduction was performed using the programs *WinXPow* (Stoe Company) for laboratory data and *GUFI* (Dinnebier, 1993) for the synchrotron data.

2.2. Commensurately modulated $Na_{1.6}CuO_2$

Commensurate $Na_{1.6}CuO_2$ crystallizes in the monoclinic crystal system with space group *Cm* and lattice parameters a = 8.228 (1), b = 13.929 (2), c = 5.707 (1) Å and β = 111.718 (2)° (Sofin *et al.*, 2005). There are 10 formula units of $Na_{1.6}CuO_2$ present in this supercell, which corresponds to Z = 2 for $Na_8Cu_5O_{10}$. The crystal structure can alternatively be described as a commensurate composite crystal within the superspace approach (van Smaalen, 2004). The first subsystem is provided by CuO_2. It has an approximate periodicity according to the basic structure unit cell of CuO_2 with $\mathbf{a}_1 = \mathbf{a}$, $\mathbf{b}_1 = (1/5)\mathbf{b}$ and $\mathbf{c}_1 = \mathbf{c}$. The second subsystem comprises Na and it has a basic structure unit cell with $\mathbf{a}_2 = \mathbf{a}$, $\mathbf{b}_2 = (1/4)\mathbf{b}$ and $\mathbf{c}_2 = \mathbf{c}$. Ribbons of CuO_2 and chains of Na atoms have

Table 2
R values of single-crystal and Rietveld refinements.

The profile *R* values as well as $R_{\rm Bragg}$ for various reflection groups are shown: all reflections, main reflections, first-order satellite reflections and second-order satellite reflections. Free refinements up to second-order harmonic modulation parameters are compared with refinements of fixed modulation parameters up to fourth order, as taken from the commensurately modulated composite structure of $Na_{1.6}CuO_2$.

	$Na_{1.6}CuO_2$	$Na_{1.62}CuO_2$		$Na_{1.58}CuO_2$	
	Free refinement	Free refinement	Commensurate modulation	Free refinement	Commensurate modulation
R_p(obs)	–	0.094	0.097	0.075	0.077
$R_{\rm wp}$(obs)	–	0.122	0.125	0.101	0.102
$R_{\rm Bragg}$(all; obs)	0.035	0.055	0.056	0.047	0.047
$R_{\rm Bragg}$(main; obs)	0.029	0.051	0.054	0.040	0.042
$R_{\rm Bragg}$(1; obs)	0.045	0.065	0.063	0.059	0.058
$R_{\rm Bragg}$(2; obs)	0.076	0.072	0.079	0.067	0.065

different periodicities along the $\mathbf{b} = 5\mathbf{b}_1 = 4\mathbf{b}_2$ direction in the ratio 5:4 (Fig. 1). This ratio is incommensurate in compounds of slightly different compositions (§2.3).

All observed reflections can be indexed with four integer indices (*hklm*) with respect to the reciprocal lattice $\{\mathbf{a}_1^*, \mathbf{b}_1^*, \mathbf{c}_1^*\}$ of the CuO_2 subsystem together with the modulation wavevector $\mathbf{q}_1 = \mathbf{b}_2^* = (4/5)\mathbf{b}_1^* = (0, 0.8, 0)$. With this indexing, the (*hkl*0) reflections are the main reflections of the CuO_2 subsystem, the (*h*0*lm*) reflections are the main reflections of the Na subsystem and the (*h*0*l*0) reflections are the main reflections common to both subsystems. The (*hklm*) reflections with $k \neq 0$ and $m \neq 0$ are satellite reflections that have non-zero intensities due to the modulations of the atomic positions of CuO_2 according to the modulation wave with wavevector $\mathbf{q}_1$, and modulations of Na according to the modulation with wavevector $\mathbf{q}_2 = \mathbf{b}_1^* = (5/4)\mathbf{b}_2^*$. Mapping the supercell structure of commensurate $Na_{1.6}CuO_2$ onto the superspace model shows that the basic structures are periodic to a good approximation for both subsystems. Shifts of the atoms out of these positions towards their true positions in the supercell are limited to 0.1 Å.

Calculations were performed using the program *JANA*2000 (Petříček *et al.*, 2000). The single-crystal data set of Sofin *et al.* (2005) was re-indexed with respect to $\mathbf{a}_1^*$, $\mathbf{b}_1^*$, $\mathbf{c}_1^*$ and $\mathbf{q}_1$. The symmetry is described by the monoclinic superspace group $C2/m(0\sigma_2 0)s0$ with $\sigma_2 = 0.8$, which was derived on the basis of the reflection conditions observed (Janssen *et al.*, 1995). The space group *Cm* of the supercell was recovered by selecting the $t_0 = 0.25$ section of superspace. Accordingly, the superspace refinements were performed in the commensurate approach, employing $t_0 = 0.25$. A superspace model for the crystal structure was developed by refinement of the basic structure against the main reflections and by the subsequent introduction of modulation parameters and refinements against the complete data set including satellite reflections. It was necessary to introduce up to fourth-order harmonic coefficients of the modulation functions of all three independent atoms of the basic structure

$$\mathbf{u}(\bar{x}_4) = \sum_{n=1}^{4} \mathbf{A}^n \sin[2\pi n\bar{x}_4] + \mathbf{B}^n \cos[2\pi n\bar{x}_4], \qquad (1)$$

with $\mathbf{A}^n = \left(A_1^n, A_2^n, A_3^n\right)$ and $\mathbf{B}^n = \left(B_1^n, B_2^n, B_3^n\right)$ being the six coefficients of the *n*th-order harmonic. The fourth superspace coordinate is $\bar{x}_4 = t + \mathbf{q}\cdot\bar{\mathbf{x}}$, with $\bar{\mathbf{x}}$ being the basic structure position of the atom and *t* the phase of the modulation wave (van Smaalen, 2004). The best fit to the diffraction data was achieved at $R = 0.062$ and $wR = 0.052$, while A_2^4 is kept equal to zero, because of high correlations between parameters. The introduction of up to fourth-order harmonic coefficients for the modulation of the anisotropic temperature parameters results in a better fit at $R = 0.035$ and $wR = 0.033$ (Table 1). The same *R* values were obtained by refinement in the fivefold supercell, but the number of parameters to achieve the same fit in the superspace approach was smaller than the number of parameters in the supercell structure (33 *versus* 40 positional and 72 *versus* 80 temperature parameters). An analysis of the modulation functions has shown that they cannot be described by crenel functions, despite the anharmonicity of the modulation (Petříček *et al.*, 1995). Parameters of the superspace model are available in the supplementary material.[1]

2.3. Rietveld refinements

LeBail fits and Rietveld refinements were performed using the program *JANA*2000, employing the incommensurate superspace approach (LeBail *et al.*, 1988; Rietveld, 1967, 1969; Dušek *et al.*, 2001). The superspace group, lattice parameters a_1, b_1, c_1 and β_1, and the basic structure coordinates of the atoms of both incommensurate Na_xCuO_2 ($x = 1.58$ and 1.62) compounds are taken from the commensurately modulated structure of $Na_{1.6}CuO_2$ (§2.2). They provide a good description of the main reflections of the CuO_2 subsystems (Fig. 2*a*). The commensurate modulation wavevector $\mathbf{q}_1 = \mathbf{b}_2^* = 0.80\mathbf{b}_2^*$ does not match the satellite reflections or the main reflections of the Na subsystem, because the latter occur at different positions for different *x* values (Fig. 2*b*). Rather, the reciprocal lattice parameters $\mathbf{b}_2^*$ of the Na subsystems were determined from the positions of the $(110\bar{1})$ reflections, that occur at approximately $2\theta = 13^\circ$ in the synchrotron data set. With these values for the lattice parameters and modulation wavevectors, LeBail-type fits proceeded smoothly with good fits to the diffraction data,

[1] Supplementary data for this paper are available from the IUCr electronic archives (Reference: CK5018). Services for accessing these data are described at the back of the journal.

while employing pseudo-Voigt profile functions with anisotropic strain broadening and an asymmetry correction according to axial divergence (Stephens, 1999; Finger *et al.*, 1994). The background was modelled by a Legendre polynomial of fifth order. An absorption correction appeared to be necessary for the laboratory data and it was applied according to the cylindrical geometry of the sample within the capillary. Anisotropic strain broadening reflects the layered structures of these compounds.

Rietveld refinements of the crystal structures start with the basic structures for each compound including isotropic temperature parameters. Harmonic parameters of the displacement modulation functions were subsequently introduced. Although third- and fourth-order harmonic coefficients, as well as anisotropic temperature parameters and their modulations, have led to lowering of the R values, the refined values of these parameters are not significant or erroneously large. Employing the same number of parameters, as appeared to be necessary for the single-crystal refinement, results in singular matrices of the Rietveld refinements for both synchrotron and laboratory diffraction data. Therefore, models with first- and second-order harmonic coefficients for displacive modulation functions together with isotropic temperature parameters were selected as the best models from the Rietveld refinements (Fig. 3). The final cycles of the refinements included variations in the lattice parameters, as well as some profile parameters (Table 1). The refined components of the modulation wavevectors $\mathbf{q}_1 = \mathbf{b}_2^* = (0, x/2, 0)$ reflect the compositions of the compounds as $x = 1.57664\ (4)$ for $Na_{1.58}CuO_2$ and $x = 1.61688\ (6)$ for $Na_{1.62}CuO_2$ (Table 1). The structural parameters are summarized in the online supplementary material.

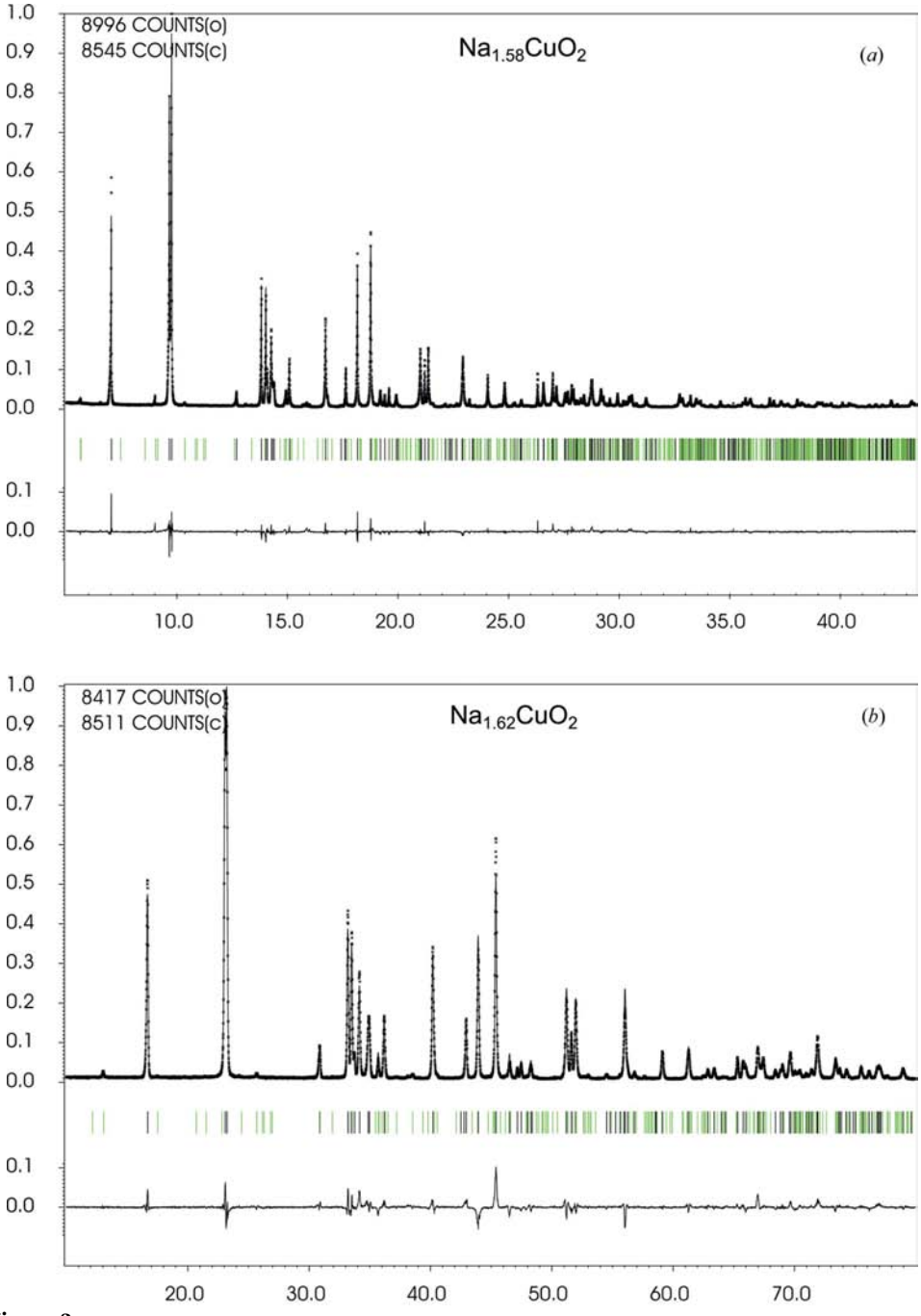

Figure 3
Scattered intensities as a function of the diffraction angle 2θ for (*a*) $Na_{1.58}CuO_2$ and (*b*) $Na_{1.62}CuO_2$. The observed patterns (diamonds), the best Rietveld-fit profiles (line), reflection markers and the difference curves between observed and calculated profiles are shown. Wavelengths are $\lambda = 0.65046$ Å for $Na_{1.58}CuO_2$ and 1.54059 Å for $Na_{1.62}CuO_2$. Black reflection markers indicate the main reflections; green (online) or grey (in print) reflection markers indicate satellite reflections.

In an alternative approach, the structural model of commensurately modulated $Na_{1.6}CuO_2$ was applied to the Rietveld refinements. Good fits to the diffraction data were obtained after the refinement of isotropic temperature parameters and the basic structure coordinates of the atoms, but with the parameters of the displacement modulations fixed at their values from the commensurate superspace model (§2.2). Attempts to refine the anisotropic temperature

Table 3
Structural parameters of Na_xCuO_2 for x = 1.6, 1.62 and 1.58.

Relative coordinates are given for the basic structure coordinates (x, y, z). Isotropic temperature parameters are given in Å^2 and modulation parameters in Å along the coordinate axes [see equation (1)].

Atom		$Na_{1.6}CuO_2$	$Na_{1.62}CuO_2$	$Na_{1.58}CuO_2$
Cu	x	0	0	0
	y	0.5	0.5	0.5
	z	0	0	0
	U_{iso}	0.0107 (1)	0.0024 (4)	0.0038 (2)
	A_1^1	−0.1179 (4)	−0.1497 (24)	−0.1398 (16)
	A_3^1	−0.1635 (3)	−0.1767 (23)	−0.1665 (15)
	B_2^2	−0.0172 (5)	−0.0064 (36)	−0.0115 (27)
	A_1^3	0.0348 (8)	–	–
	A_3^3	0.0152 (9)	–	–
	B_2^4	−0.0038 (9)	–	–
O	x	0.0520 (1)	0.0526 (3)	0.0493 (3)
	y	0	0	0
	z	0.2423 (1)	0.2465 (5)	0.2416 (3)
	U_{iso}	0.0161 (2)	0.0208 (10)	0.0091 (7)
	A_1^1	0.0983 (14)	0.0304 (72)	0.0968 (54)
	B_2^1	0.0667 (13)	0.0619 (67)	0.0901 (52)
	A_3^1	0.1390 (11)	0.1031 (66)	0.1329 (48)
	B_1^2	−0.0500 (22)	−0.031 (12)	0.030 (10)
	A_2^2	0.0567 (21)	0.028 (10)	0.057 (9)
	B_3^2	−0.0431 (19)	0.042 (13)	0.043 (10)
	A_1^3	0.0630 (39)	–	–
	B_2^3	−0.0228 (29)	–	–
	A_3^3	0.0245 (35)	–	–
	B_1^4	0.0105 (58)	–	–
	A_2^4	0.0133 (37)	–	–
	B_3^4	0.0020 (55)	–	–
Na	x	−0.1542 (1)	−0.1566 (4)	−0.1512 (3)
	y	0.25	0.25	0.25
	z	0.3779 (1)	0.3717 (5)	0.3832 (4)
	U_{iso}	0.0268 (3)	0.0183 (9)	0.0141 (6)
	B_1^1	−0.2998 (12)	−0.3265 (45)	−0.2947 (41)
	A_2^1	0.3430 (14)	0.3486 (40)	0.3928 (33)
	B_3^1	−0.1463 (11)	−0.1897 (53)	−0.1332 (42)
	B_1^2	−0.0673 (18)	−0.1726 (71)	−0.1653 (72)
	A_2^2	−0.0061 (19)	0.0098 (73)	0.0565 (54)
	B_3^2	−0.0554 (17)	−0.1088 (88)	−0.1014 (70)
	B_1^3	0.0346 (33)	–	–
	A_2^3	−0.0624 (25)	–	–
	B_3^3	−0.0041 (35)	–	–
	B_1^4	0.0194 (30)	–	–
	A_2^4	0	–	–
	B_3^4	0.0023 (26)	–	–

parameters or their modulations have failed. Final R values are summarized in Table 2.

3. Discussion

Crystal structures are reported for three different Na_xCuO_2 compounds, employing three different experimental techniques: single-crystal X-ray diffraction for a commensurate compound with x = 1.6, synchrotron-radiation X-ray powder diffraction for an incommensurate compound with x = 1.58, and X-ray powder diffraction with Cu $K\alpha_1$ radiation for an incommensurate compound with x = 1.62. The standard uncertainties (s.u.s) of the modulation parameters indicate that single-crystal diffraction is by far the most accurate method, while powder diffraction with radiation from an X-ray tube provides the least accurate structure model, in accordance with expectations (Table 3).

The commensurate and incommensurate Na_xCuO_2 compounds are not necessarily described by the same structural parameters, although the unified superspace approach supports the idea that different compounds should be described by similar basic structures and similar modulation functions. Similarities were indeed found, but the refined values of the modulation parameters exhibit differences well beyond three times their s.u.s. However, the application of Berar's factor of approximately 4 to the s.u.s of the parameters from the Rietveld refinements makes all the differences less than three times their s.u., at the expense of large uncertainties for the modulation parameters of up to 0.02 Å for $Na_{1.58}CuO_2$ and up to 0.03 Å for $Na_{1.62}CuO_2$ (Table 3). A further indication of the similarities of the modulations of the three compounds can be seen from the calculated diffraction patterns for the incommensurate structures employing the modulation parameters of commensurate $Na_{1.6}CuO_2$, which fit

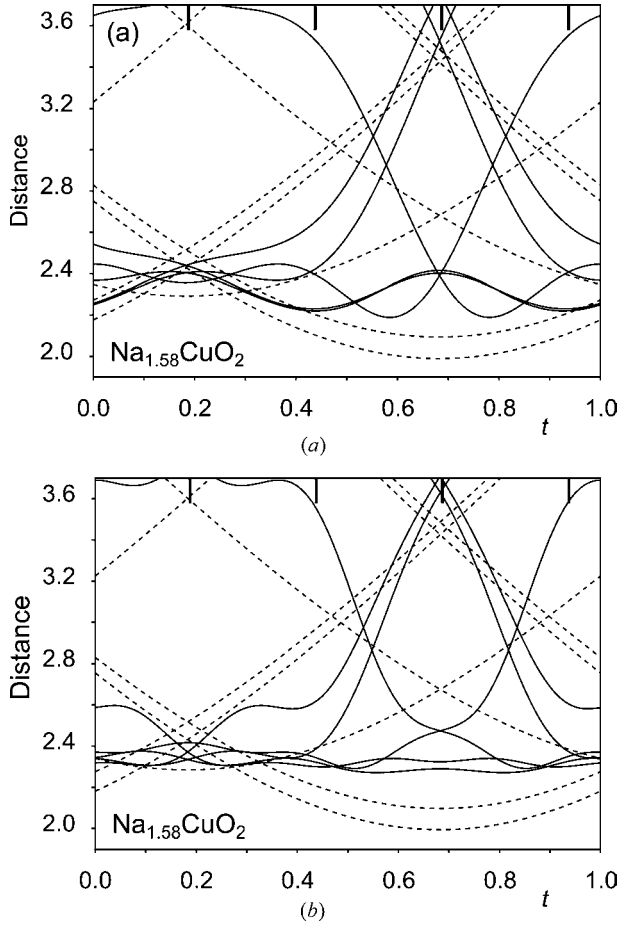

Figure 4
Coordination of Na by O in $Na_{1.58}CuO_2$. (*a*) Refined modulation functions; (*b*) modulation functions from $Na_{1.6}CuO_2$. The bond distances between Na and O as a function of the incommensurate parameter t are shown. The full and dashed lines apply to the modulated and basic structures, respectively. The t values representing the coordinations of Na in commensurate $Na_{1.6}CuO_2$ are indicated by vertical bars at t = 0.1875, 0.4375, 0.6875 and 0.9375.

Table 4
Average atomic valences in the incommensurate structures of $Na_{1.58}CuO_2$ and $Na_{1.62}CuO_2$.

Valences were computed by the bond-valence method with parameters R_0[Na—O] = 1.800 Å and R_0[Cu—O] = 1.7133 Å obtained as the average parameters of Cu^{2+} and Cu^{3+} according to Brese & O'Keeffe (1991).

	$Na_{1.62}CuO_2$		$Na_{1.58}CuO_2$	
	Free refinement	Commensurate modulation	Free refinement	Commensurate modulation
Na	1.03	1.01	1.03	1.01
Cu	2.31	2.31	2.45	2.44
O	1.99	1.97	2.04	2.02

the diffraction data almost as well as the refined modulation parameters (Table 2).

The basic structures of composite crystals are fictitious structures, because displacive modulations are necessary to arrive at chemically stable environments of the atoms. The ribbons of CuO_2 are more rigid than the chains of the Na atoms, with the result that the largest modulations are found for the Na atoms (Table 3). Atomic coordinations can be studied by so-called *t* plots (van Smaalen, 2004). Modulations of Na are such that they lead to nearly constant values of the shortest Na—O distances, *i.e.* the strongest Na—O bonds (Fig. 4*a*). Assuming a single most stable coordination of Na by O, the modulation of commensurate $Na_{1.6}CuO_2$ provides a better description of the modulations of the incommensurate compounds, because it leads to smaller variations of the shortest Na—O distances than is obtained for the two-harmonic model (Fig. 4*b*). The stable environments of Na are reflected in the valences as computed by the bond-valence method (Brown, 2002; Brese &O' Keeffe, 1991). The average values are approximately 1 for both structure models (Table 4), while the variation of *t* is smaller for the four-harmonic model (Fig. 5).

Modulations of Cu and O are of comparable magnitude; they define undulating ribbons (Fig. 1). Copper is coordinated

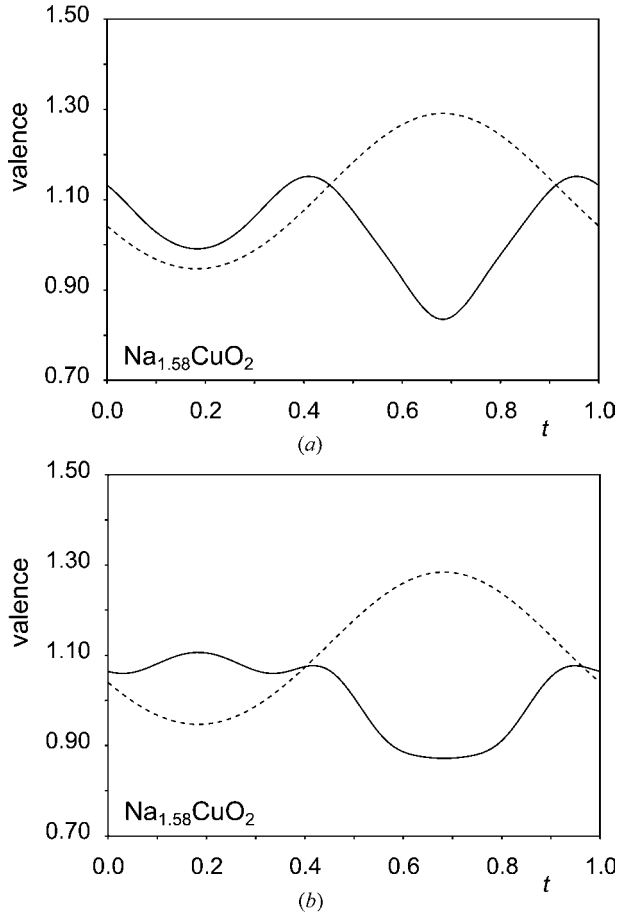

Figure 5
The valence of Na in $Na_{1.58}CuO_2$. (*a*) Refined modulation functions; (*b*) modulation functions from $Na_{1.6}CuO_2$. Valences have been computed by the bond-valence method with the parameter R_0[Na—O] = 1.800 Å (Brese & O'Keeffe, 1991). Full and dashed lines apply to modulated and basic structures, respectively.

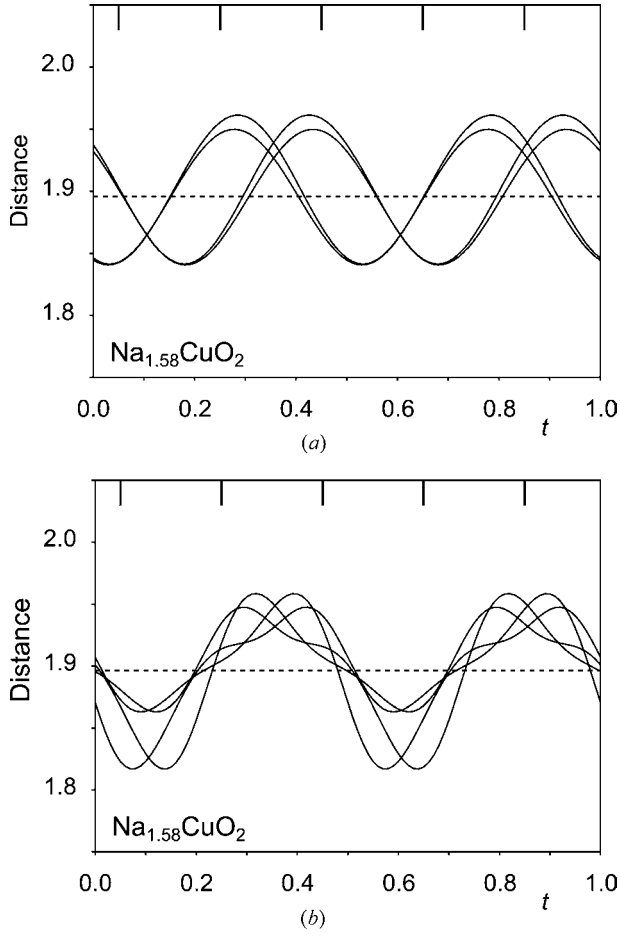

Figure 6
Coordination of Cu by O in $Na_{1.58}CuO_2$. (*a*) Refined modulation functions; (*b*) modulation functions from $Na_{1.6}CuO_2$. The full and dashed lines apply to modulated and basic structures, respectively. The *t* values representing the coordinations of Cu in commensurate $Na_{1.6}CuO_2$ are indicated by vertical bars at *t* = 0.05, 0.25, 0.45, 0.65 and 0.85.

by four O atoms that occur at single distances in the basic structures. Relatively large variations of the Cu—O bond length are observed in the modulated structure (Fig. 6). They reflect modulations of Cu and O that have a large out-of-phase component. The origin of the dependence of the Cu—O bond length on t is the presence of both Cu^{2+} and Cu^{3+}, as it is reflected in the computed valences (Fig. 7). The sequence of Cu^{2+} and Cu^{3+} is the same as that found from the supercell refinement of $Na_{1.6}CuO_2$ (Fig. 8; Sofin *et al.*, 2005). The modulation derived from commensurate $Na_{1.6}CuO_2$ represents larger variations of the valence of Cu than the two-harmonic model (Fig. 7), again suggesting the former to be more accurate.

The results obtained on the commensurate (x = 1.6) as well as the incommensurate structures (x = 1.58 and 1.62) can be rationalized consistently and on a crystal chemically and physically meaningful basis. In the parent $NaCuO_2$ compound ribbons are tilted such that one almost regular octahedral site for sodium per copper atom results (Fig. 8). For the mixed-valent cuprates, the CuO_2 strands are rotated by *ca* 15° compared with $NaCuO_2$, which produces enlarged and significantly elongated octahedra. This arrangement then offers at least three different oxygen environments to accommodate sodium: square pyramidal, tetrahedral and triangular. More importantly, the freedom to incorporate additional sodium ions is generated, which is one of the prerequisites for an electron doping on the Cu sublattice. Using $Na_{1.6}CuO_2$ (Fig. 8*a*) as an example, it is possible to visualize how the modulation in this part of the crystal structure evolves in general.

The compositions are directly related to the modulation wavevectors, as accurately determined from the powder

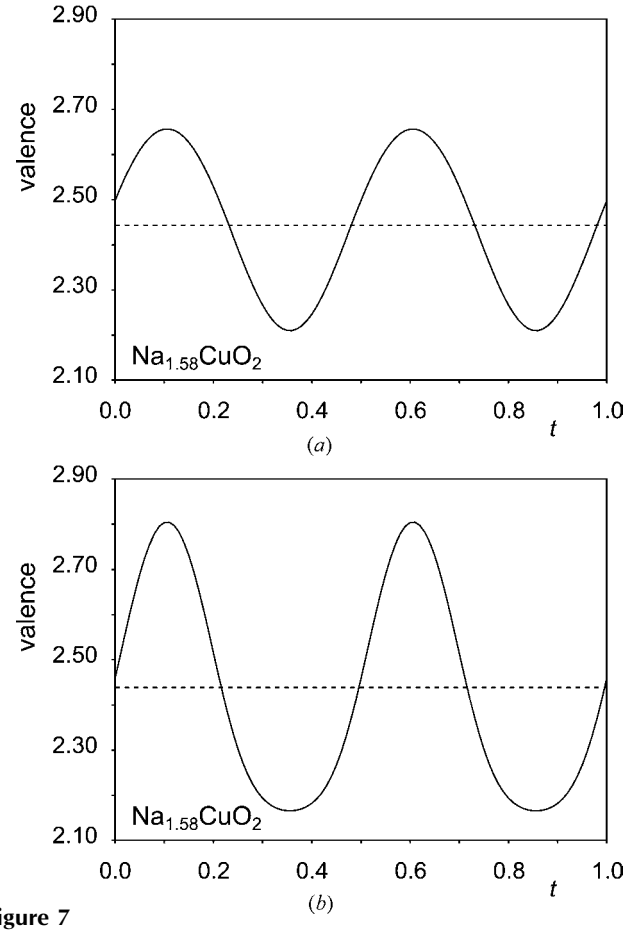

Figure 7
Valence of Cu in $Na_{1.58}CuO_2$. (*a*) Refined modulation functions; (*b*) modulation functions from $Na_{1.6}CuO_2$. Valences have been computed by the bond-valence method with the parameter R_0[Cu—O] = 1.7133 Å obtained as the average of the parameters of Cu^{2+} and Cu^{3+} according to Brese & O'Keeffe (1991). Full and dashed lines apply to the modulated and basic structures, respectively.

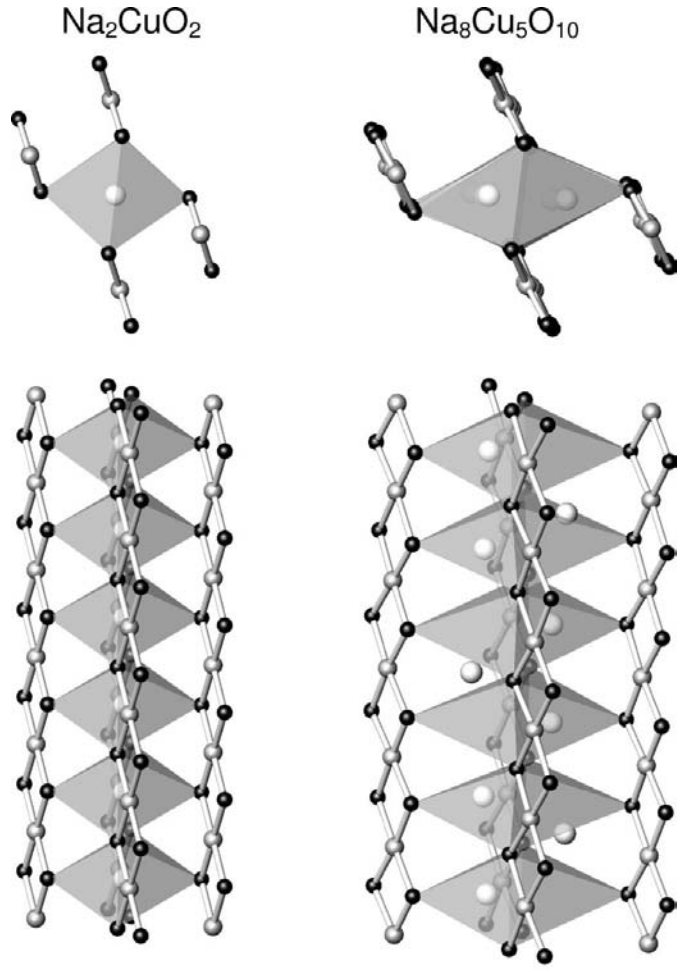

Figure 8
Positions of the Na atoms in (*a*) Na_2CuO_2 and (*b*) in $Na_8Cu_5O_{10}$, demonstrating the evolution of a displacive modulation in the latter.

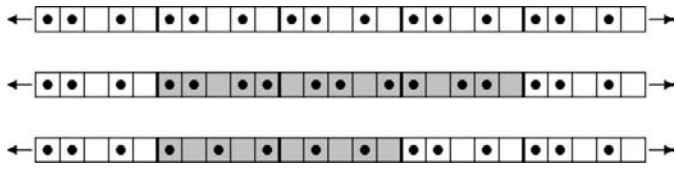

Figure 9
Charge-ordering patterns of the copper ions: (top) undisturbed in $Na_8Cu_5O_{10}$, (middle) defect region increasing the electron doping by one, and (bottom) defect region decreasing the electron doping by one. Dots: electron-doped (Cu^{2+}) sites, grey background: defect regions.

diffraction data. For the partial copper structures of $Na_{1.58}CuO_2$ and $Na_{1.62}CuO_2$ this means that out of 50 Cu atoms in $Na_{1.60}CuO_2$ just one has to change its ionic charge from 2+ to 3+, and 3+ to 2+, respectively. Since $Na_3Cu_2O_4$ and $Na_8Cu_5O_{10}$ have been shown to represent Wigner crystals (Horsch *et al.*, 2005), it appears to be justified to also assume integral charges for copper in the incommensurate structures. Given these boundary conditions, it is understandable that for all three structures the commensurate pattern $Cu^{2+}/Cu^{2+}/Cu^{3+}/Cu^{2+}/Cu^{3+}$ has been found in the experiments. The slight changes in charge can be regarded as local defects that even after relaxation show a maximal extension of 42 Å along the chain (Fig. 9). The energy needed to produce these defects will be rather low.

Modulations in Na_xCuO_2 ($x \simeq 1.6$) are different from modulations in Ca_yCuO_2 ($y \simeq 0.83$), with small displacements of Ca and large displacements of O in the latter compound (Miyazaki *et al.*, 2002). This difference can be understood from the different stacking of the ribbons of CuO_2 in the two compounds, which led to an environment of Na that is more flexible than the environment provided by the higher coordination numbers of Ca (Fig. 1). An increased flexibility of the atomic chains in Na_xCuO_2 might also be responsible for the fact that Na_xCuO_2 can be synthesized for different compositions of x, as shown by the dependence of the lattice parameter b_2 on the sample (Fig. 2). The driving force leading to a particular composition is the chemical potential, as defined by the relative quantities of elements in the closed container during synthesis. Different quantities of Na are then easily accommodated in the structure by variations in the modulations.

4. Conclusions

Na_xCuO_2 ($x \simeq 1.6$) has been synthesized for different compositions of x, resulting in both commensurate and incommensurate composite crystals (Fig. 2). The structures of two incommensurate compounds ($x = 1.58$ and $x = 1.62$) and commensurate $Na_8Cu_5O_{10}$ ($x = 1.6$) are found to be similar. Valence fluctuations of Cu^{2+}/Cu^{3+} are at the origin of the modulations of the CuO_2 subsystems (Fig. 7), while displacive modulations of Na are defined by the closest Na—O contacts between the subsystems (Fig. 4). The fact that the Cu^{2+}/Cu^{3+} modulation remains virtually invariant could be explained by stoichiometric deviations caused by local defects.

The structural differences observed might reflect the different modulations and different average periodicities of the subsystems as required by the different compositions of Na_xCuO_2. However, the differences are not larger than the relatively large standard uncertainties of the modulation parameters obtained by the Rietveld refinements of the incommensurate compounds. The present results thus provide one more illustration of the fact that much higher accuracies of structural parameters can be achieved by single-crystal X-ray diffraction than that which can be obtained from Rietveld refinements against X-ray powder diffraction data (Dušek *et al.*, 2001).

We thank P. Stephens for assistance with synchrotron-radiation X-ray diffraction at beamline X3B1 of the National Synchrotron Light Source (NSLS) at Brookhaven National Laboratory. Financial support was obtained from the German Science Foundation (DFG) and the Fonds of the Chemical Industry (FCI).

References

Brese, N. E. & O'Keeffe, M. (1991). *Acta Cryst.* B**47**, 192–197.
Brown, I. D. (2002). *The Chemical Bond in Inorganic Chemistry; The Bond Valence Method*. Oxford University Press.
Dinnebier, R. E. (1993). *GUFI, Program for Measurement and Evaluation of Powder Pattern*. Heidelberger Geowiss. Abh., Vol. 68. ISBN 3–89257-067–1.
Dušek, M., Petříček, V., Wunschel, M., Dinnebier, R. E. & van Smaalen, S. (2001). *J. Appl. Cryst.* **34**, 398–404.
Finger, L. W., Cox, D. E. & Jephcoat, A. P. (1994). *J. Appl. Cryst.* **27**, 892–900.
Horsch, P., Sofin, M., Mayr, M. & Jansen, M. (2005). *Phys. Rev. Lett.* **94**, 076403.
Janssen, T., Janner, A., Looijenga-Vos, A. & de Wolff, P. M. (1995). *International Tables for Crystallography*, Vol. C, edited by A. J. C. Wilson, pp. 797–835. Dordrecht: Kluwer Academic Publishers.
LeBail, A., Duroy, H. & Fourquet, J. L. (1988). *Mater. Res. Bull.* **23**, 447–452.
Miyazaki, Y., Onoda, M., Edwards, P. P., Shamoto, S. & Kajitani, T. (2002). *J. Solid State Chem.* **163**, 540–545.
Petříček, V., Dušek, M. & Palatinus, L. (2000). *JANA*2000. Institute of Physics of the Czech Academy of Sciences, Praha, Czech Republic.
Petříček, V., van der Lee, A. & Evain, M. (1995). *Acta Cryst.* A**51**, 529–535.
Rietveld, H. M. (1967). *Acta Cryst.* **22**, 151.
Rietveld, H. M. (1969). *J. Appl. Cryst.* **2**, 65.
Siegrist, T., Roth, R. S., Rawn, C. J. & Ritter, J. J. (1990). *Chem. Mater.* **2**, 192–194.
Smaalen, S. van (1999). *Z. Kristallogr.* **214**, 786–802.
Smaalen, S. van (2004). *Z. Kristallogr.* **219**, 681–691.
Sofin, M., Peters, E.-M. & Jansen, M. (2005). *J. Solid State Chem.* **178**, 3708–3714.
Stephens, P. W. (1999). *J. Appl. Cryst.* **32**, 281–289.
Tokura, Y. & Nagaosa, N. (2000). *Science*, **288**, 462–468.